China Geology 7 (2024) 505−516

China Geology

Journal homepage: http://chinageology.cgs.cn
https://www.sciencedirect.com/journal/china-geology

Depositional process of hyperpycnal flow deposits: A case study on Lower Cretaceous Sangyuan outcrop in the Luanping Basin, Northeast China

De-zhi Yan[a,*], Ru-kai Zhu[a, b, c], Hao Shou[a], Zhao-hui Xu[d, e], Wei-hong Liu[a], Si-cheng Zhu[e], Zhi-cheng Lei[f], Jing-ya Zhang[a], Chang Liu[a], Yi Cai[a], Huai-min Xu[d, e]

[a] *Research Institute of Petroleum Exploration and Development*, *PetroChina*, *Beijing* 100083, *China*
[b] *National Energy Tight Oil and Gas R & D Center*, *Beijing* 100083, *China*
[c] *PetroChina Key Laboratory of Oil and Gas Reservoir*, *Beijing* 100083, *China*
[d] *State Key Laboratory of Petroleum Resources and Prospecting*, *China University of Petroleum (Beijing)*, *Beijing* 102249, *China*
[e] *College of Geosciences*, *China University of Petroleum (Beijing)*, *Beijing* 102249, *China*
[f] *Jiangxi Engineering Laboratory on Radioactive Geoscience and Big Data Technology*, *Department of Information and Engineering*, *East China University of Technology*, *Nanchang* 330013, *China*

ARTICLE INFO

Article history:
Received 27 August 2023
Received in revised form 27 October 2023
Accepted 24 November 2023
Available online 1 April 2024

Keywords:
Hyperpycnal flow
Sedimentary characteristics
Depositional process
Gravity flow deposit
Hyperpycnite
Red mud pebble
Gray mud pebble
Oil and gas exploration engineering
Luanping Basin

ABSTRACT

Sedimentary process research is of great significance for understanding the distribution and characteristics of sediments. Through the detailed observation and measurement of the Sangyuan outcrop in Luanping Basin, this paper studies the depositional process of the hyperpycnal flow deposits, and divides their depositional process into three phases, namely, acceleration, erosion and deceleration. In the acceleration phase, hyperpycnal flow begins to enter the basin nearby, and then speeds up gradually. Deposits developed in the acceleration phase are reverse. In addition, the original deposits become unstable and are taken away by hyperpycnal flows under the eroding force. As a result, there are a lot of mixture of red mud pebbles outside the basin and gray mud pebbles within the basin. In the erosion phase, the reverse deposits are eroded and become thinner or even disappear. Therefore, no reverse grading characteristic is found in the proximal major channel that is closer to the source, but it is still preserved in the middle branch channel that is far from the source. After entering the deceleration phase, normally grading deposits appear and cover previous deposits. The final deposits in the basin are special. Some are reverse, and others are normal. They are superimposed with each other under the action of hyperpycnal flow. The analysis of the Sangyuan outcrop demonstrates the sedimentary process and distribution of hyperpycnites, and reasonably explain the sedimentary characteristics of hyperpycnites. It is helpful to the prediction of oil and gas exploration targets in gravity flow deposits.

1. Introduction

Subaqueous gravity flow (Middleton GV and Hampton MA, 1973), such as debris flow and turbulent flow, is a key transport mechanism for supplying deposits to submerged basins (Henstra GA et al., 2016). Based on the triggering mechanism, gravity flow can be divided into two types: Slump-derived gravity flow and flood-induced gravity flow (hyperpycnal flow) (Walker RG, 1978). Slump-derived gravity flow is the result from the secondary transport of deposits in a basin (Shanmugam G, 2019). A lot of researches have been done on the mechanism, sedimentary process and characteristics of slump-derived gravity flow (Middleton GV, 1976; Lowe DR, 1982; Soyinka OA and Slatt RM, 2008; Shanmugam G, 2019). Theories associated with slump-derived gravity flow have been widely applied to research lacustrine gravity flow over the past few decades (Shanmugam G, 2000; Zou CN et al., 2012; Cao YC et al., 2017).

Hyperpycnal flow was defined as a density outflow from river mouth due to its higher density than that of the fluid where it flows (Bates CC, 1953). So hyperpycnal flow is a density flow running on the bottom of the basin that develops with river flood events (Bates CC, 1953; Zavala C, 2018).

* Corresponding author: *E-mail address*: ydz920859212@126.com (De-zhi Yan).

Literary editor: Li-qiong Jia
doi:10.31035/cg2023096
2096-5192/© 2024 China Geology Editorial Office.

Some criterions for the formation of hyperpycnal flow have been established after studying marine hyperpycnal flow (Parsons JD et al., 2001; Warrick JA and Milliman JD, 2003; Dadson S, 2005; Peter AL and Steel RJ, 2006; Lamb MP and Mohrig D, 2009; Pierdomenico M et al., 2019; Zavala C et al., 2018, 2020). According to the criterions, some experts believe that rivers around mountains are prone to trigger hyperpycnal flow, especially in areas where rifted lacustrine basins developed (Wu FD et al., 2004). Some studies believed that flood developing process had a controlling effect on the sedimentary characteristics of hyperpycnites (Lamb MP and Mohrig D, 2009; Pierdomenico M, 2019). The typical sedimentary rhythm of hyperpycnites is composed of a reverse grading basal unit deposited during the waxing period of discharge, a normal grading top unit deposited during the waning period of discharge, and an erosion surface between the two units (Mulder T et al., 2003; Zavala C et al., 2006; Yan DZ et al., 2020). Hyperpycnites differ from other gravity flow deposits because of their well-developed and reversely grading facies and intra-sequence erosional contacts (Mulder T et al., 2003). A hyperpycnal flow sedimentary model was established by Yan DZ et al., (2020), including three segments: Proximal major channel deposits (FAA), middle branch channel deposits (FAB), and distal lobe deposits (FAC). Hyperpycnal flow has changed the traditional concept of sediment transport. In addition, due to its complexity, hyperpycnal flow has attracted many researchers to study its various aspects, both experimentally and theoretically (Khan SM et al., 2005; Peter AL and Steel RJ, 2006; Lamb MP and Mohrig D, 2009; Pierdomenico M et al., 2019). Although the concept of hyperpycnal flow was proposed very early, there are few comprehensive and systematic studies on it. A lot of researches on the sedimentary characteristics and models of hyperpycnites have been done (Parsons JD et al., 2001; Dadson S et al., 2005; Peter AL and Steel RJ, 2006; Pierdomenico M, 2019; Zavala C et al, 2018, 2020; Yan DZ et al., 2020), but its depositional process is still unclear.

This study conducted field observation on the Sangyuan outcrop to investigate the depositional process of the hyperpycnal flow. The depositional process of individual hyperpycnites in a complete flooding cycle from waxing to waning phases were analyzed. The purpose of the study is to further understand the behavior of the hyperpycnal flow running into the basin. The findings provide new insights into the depositional process that generate hyperpycnites in continental rifted basins, and may shed new light on the sedimentary system investigated in submerged basins.

2. Geological setting

The Luanping Basin is a typical rifted lacustrine basin where a large amount of gravity flow sediments have developed (Li Y, 2003; Zhang YL et al., 2007; Cope T et al., 2010). The outcrop, namely the Cretaceous Sangyuan section, is located at the northwest of the Luanping Basin (Fig. 1a). The Early Cretaceous period was characterized by strong tectonic activities, major topographic differences, humid climate, a vast lacustrine basin, and abundant sediment supply, which provided favourable conditions for the development of hyperpycnal flow deposits (Wu FD et al., 2004). The Sangyuan section extends in the NWN-SES direction, longer than 1300 m and as high as 163 m (Fig. 1b).

The deposits are composed of a successive combination of conglomerate, coarse sandstone, medium sandstone, fine sandstone, siltstone and mudstone, and have abundant phytodetritus, massive bedding, imbricated structure, cut-and-fill structure, asymmetrical cross laminae, climbing ripples, parallel laminae, horizontal bedding. The grains gradually become finer from WNW to ESE, and the long axis of the gravels extends approximately SW-NE (Fig. 2b), which suggests that the flow was from south-west to north-east (Cope T et al., 2003; Yan DZ et al., 2020). They are a complex of a reverse grading basal unit and a normal grading top unit with an erosion surface between the two units (Fig. 3c). The color of the mudstone is almost black (Fig. 4d), which reflects that the sedimentary environment was reducing, maybe a deeper basin (lake) during the depositional stage (Yan DZ et al., 2020).

Some previous studies suggested that the Sangyuan section is composed of fan delta deposits (Wu FD et al., 2004; Er C et al., 2010), but they did not give a reasonable explanation for this special sedimentary characteristic, the superposition of a reverse grading basal unit and a normal grading top unit with internal erosion surfaces between them. The recurrence of reverse and normal grading, and multiple internal erosion surfaces reflect fluctuations in flow rate. It is also a remarkable characteristic of hyperpycnal flow deposits (Mulder T et al., 2003). The research results also mentioned a similar sedimentary characteristic (Fig. 3d), and attributed it to hyperpycnites (Mulder T et al., 2003; Yang RC et al., 2015; Zavala C et al., 2006, 2018, 2020). They believed that because the hyperpycnal flow accelerated to the flood peak at first and then decelerated, the resulting sediments are featured by the superposition of reverse and normal grading units with internal erosion surfaces between them. Therefore, we infer that the Sangyuan section was generated by fluvial discharges into the lake as hyperpycnal flow.

3. Data and methods

The Sangyuan outcrop is about 1300 m long and 163 m high. Detailed observations are made along the Sangyuan Section. Architectural dimensions, such as the length and height of the section, as well as the channel length and thickness were collected using a laser range finder with 0.1 m resolution and 0.3 m accuracy for distance measurement. Stratigraphic section was measured, totally 260 m thick, at 0.1 m resolution. The composition of the sediments is calculated using measured data, including conglomerate, coarse, medium and fine sandstone, siltstone, and shale, totally more than 260 m thick. Furthermore, more than 300 photographs with high resolution were collected to study the sedimentary structure of

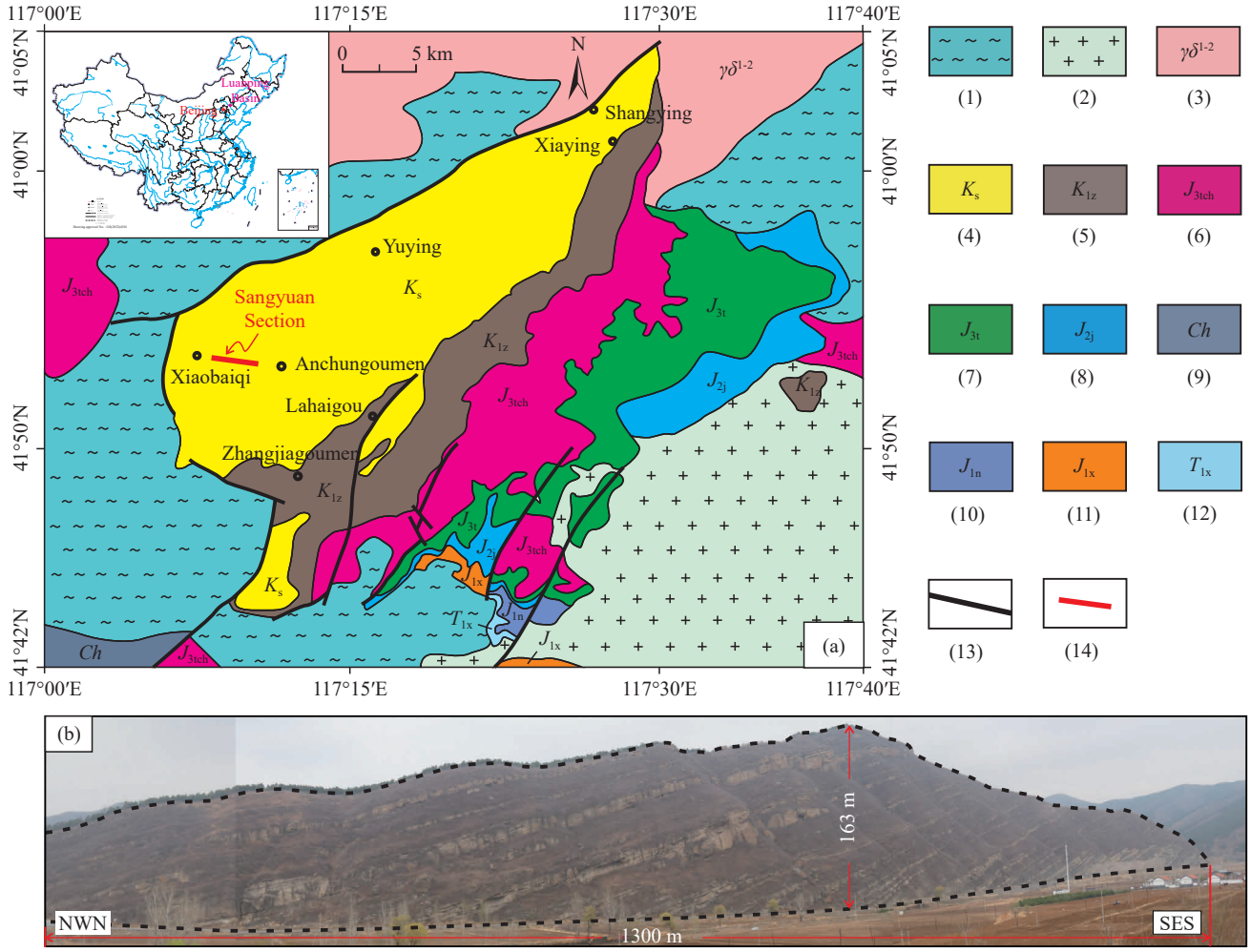

Fig. 1. Location and geological map of the Luanping Basin, demonstrating the stratigraphic distribution, bounding fault, and location of Sangyuan outcrop (a), and length, height and strike of the Sangyuan Section (b). 1–Archaeozoic; 2–Cretaceous intrusive rock; 3–granitic diorite; 4–undivided Lower Cretaceous sediments (large Xiguayuan Formation); 5–Zhangjiakou Formation; 6–Tuchengzi Formation; 7–Tiaojishan Formation; 8–Jiulongshan Formation; 9–Changcheng System; 10–Nandaling Formation; 11–Xihuayuan Formation; 12–Xingshikou Formation; 13–fault; 14–Sangyuan section.

the Sangyuan Section. Layer thickness, grain size and color are used to study the lateral and vertical trends. Classification of facies and facies associations are based on the depositional features of the studied facies. The observed facies and facies associations were used to infer depositional processes.

4. Sedimentologic characterization of hyperpycnites

Based on sedimentological characteristics, such as grain size, color, and thickness, eight lithofacies (F) and three facies associations (FA) are identified in the Sangyuan Section to define the depositional environment and sedimentary process. The lithofacies description and interpretation are summarized in Table 1. The sedimentary structures of these facies association represent the occurrences of hyperpycnites and different sedimentary processes.

4.1. Facies association A

Facies association A (FAA) is massive and imbricated conglomerate (F1 in Table 1) with medium-fine sandstone matrix in the middle. It is a sandy matrix-supported structure. FAA has a lenticular shape, thick in the middle and thin on both ends (Fig. 2a). This facies association has normal graded bedding, 1 m to 5 m thick. Significant amounts of gravels with poorly sortable and poorly round sediments with diameters of 1 m to 15 cm are deposited at the bottom of FAA. The long axis of the gravels extends approximately SW-NE (Fig. 2b). The colors are variable. Red and grey conglomerate is mixed with black and dark grey mud pebbles (Fig. 2d). FAA exhibits the effects of erosion on the lower mudstone or sandstone, shown as flute casts (Fig. 2c). The amalgamated thickness is around 2 m to 15 m, and thin black or greyish-green silty mudstone and mudstone are found in FAA (Fig. 2a). Each interlayer is 0 m to 25 cm, with poor lateral continuity. The thickness of the silty mudstone and the mudstone interlayer reduces as the thickness of the sandstone increases.

The gravels in FAA are deposited in a specific direction, with signs of imbrication. It is inferred that the coarser sediments are bedload transported at the time of deposition. The direction of the long axis of these gravels suggests that

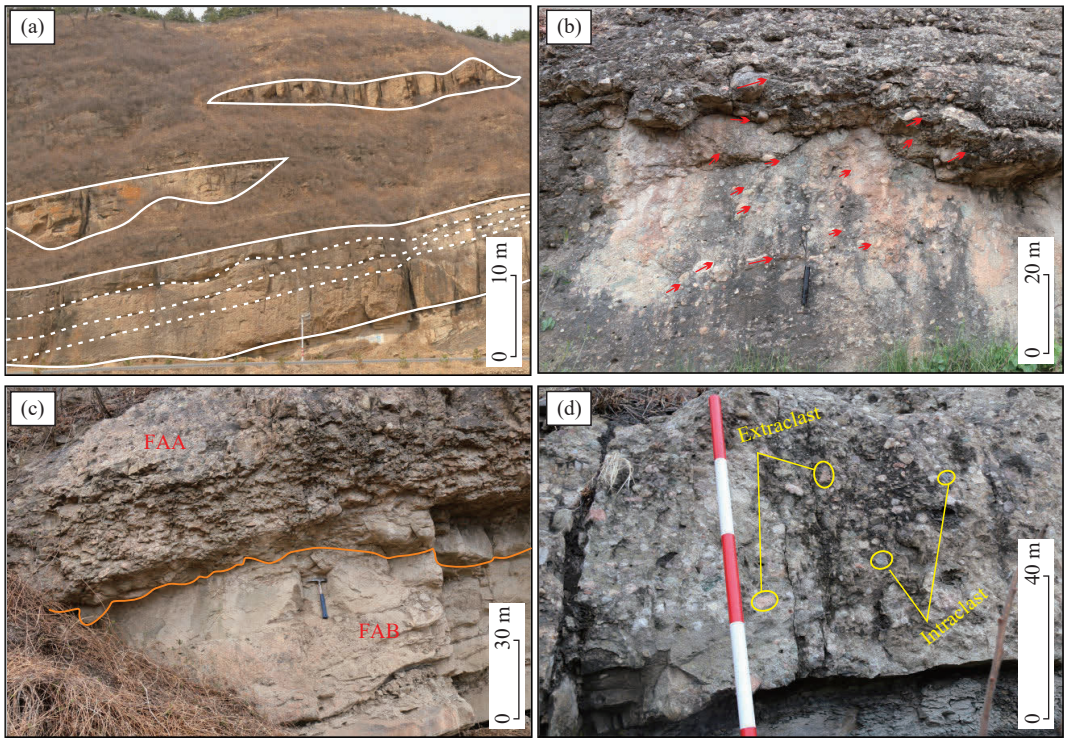

Fig. 2. FAA examples of proximal main channel deposits (modified from Yan DZ et al., 2020). a–outlines (flat top and flanged bottom) and dividing lines of main channels (white); b–directional gravels at the bottoms of main channels; c–erosion on mudstone or sandstone, and flute casts; d–red and grey conglomerates are mixed with black and dark grey mud pebbles.

the direction of the flood was from south-west to north-east, which is consistent with the results of Zhang YL et al., (2007). The middle-fine sandstone is interpreted as the sediment load carried in suspension by the flow. The amalgamated sandstone is interpreted as channel deposits, because of the "flat top and flanged bottom" outlines. FAA is characterized by coarse sediments, with poorly sortable and poorly round gravels, suggesting that FAA sediments should have been closer to the sediment source. The thin black and greyish-green mudstone at the top of the sandstone was deposited when the flood hydrodynamic force became weak, and the unequal thickness of the mudstone represents that late channel deposits eroded the earlier. Moreover, the analysis of the channel deposits suggests that erosion became stronger on the meandric deposit belt. As a result, the mudstone interlayer becomes thicker from the center to both sides of the channel. The colours of the mudstone changing from black to greyish-green represents a reducing environment that corresponds to a deeper basin (lake). The mixed colour of the gravels in FAA represents that extraclasts are mixed with interaclasts, which is consistent with the observations of Zavala C and Arcuri M (2016) and Xian BZ et al. (2018).

As previously mentioned, three depositional phases, acceleration, erosion + bypass, and deceleration, exist in a single long-life hyperpycnal flow (Zavala C et al., 2006), corresponding to three kinds of sedimentary phenomena, i.e., normal bedding, erosional surface, and reverse bedding on the vertical profile (Zavala C et al., 2006; Yang RC et al., 2015; Sun FN et al., 2016). However, in FAA of the Sangyuan outcrop, only normal bedding and erosional surfaces are observable (Fig. 2a). This suggests that early reverse bedding has been eroded under strong flood forces.

4.2. Facies association B

Facies association B (FAB) is medium-coarse sandstone with massive bedding, graded bedding, cross bedding, parallel bedding and climbing bedding, with dispersed 1–5 cm gravels, (F2 to F6 in Table 1). FAB is poorer than FAA in roundness and sortability. In FAB, red conglomerates and greyish-green mud pebbles are mixed (Fig. 3b); a large number of plant fragments are observed (Figs. 3d, e); a complete vertical section of the deposits from a single hyperpycnal flow is found, including normal bedding, erosional surface, and reverse bedding (Figs. 3c, d); and a large amount of gravels with directional arrangement are recognised in the proximity of the erosional surface (Figs. 3c, d). The direction of the long axis of the gravels is approximately SW-NE, which is similar to FAA. The amalgamated sandstone is 0.5 m to 3 m thick, where alternative occurrences of cross bedding and parallel bedding are identifiable on the profile (Fig. 3a). There are flute clasts at the bottom of FAB (Fig. 3f).

Compared to FAA, the gravels in FAB are finer, much rounder and more sortable, suggesting that FAB is farther from the source. A complete sedimentological architecture that's associated with a single hyperpycnal flow is observable on FAB profiles, exhibiting a weaker hydrodynamic hyperpycnal flow than FAA, and early reverse deposits. Additionally, on the vertical profiles, a coarsening-upward bottom unit, erosional surfaces, and a fining-upward top unit

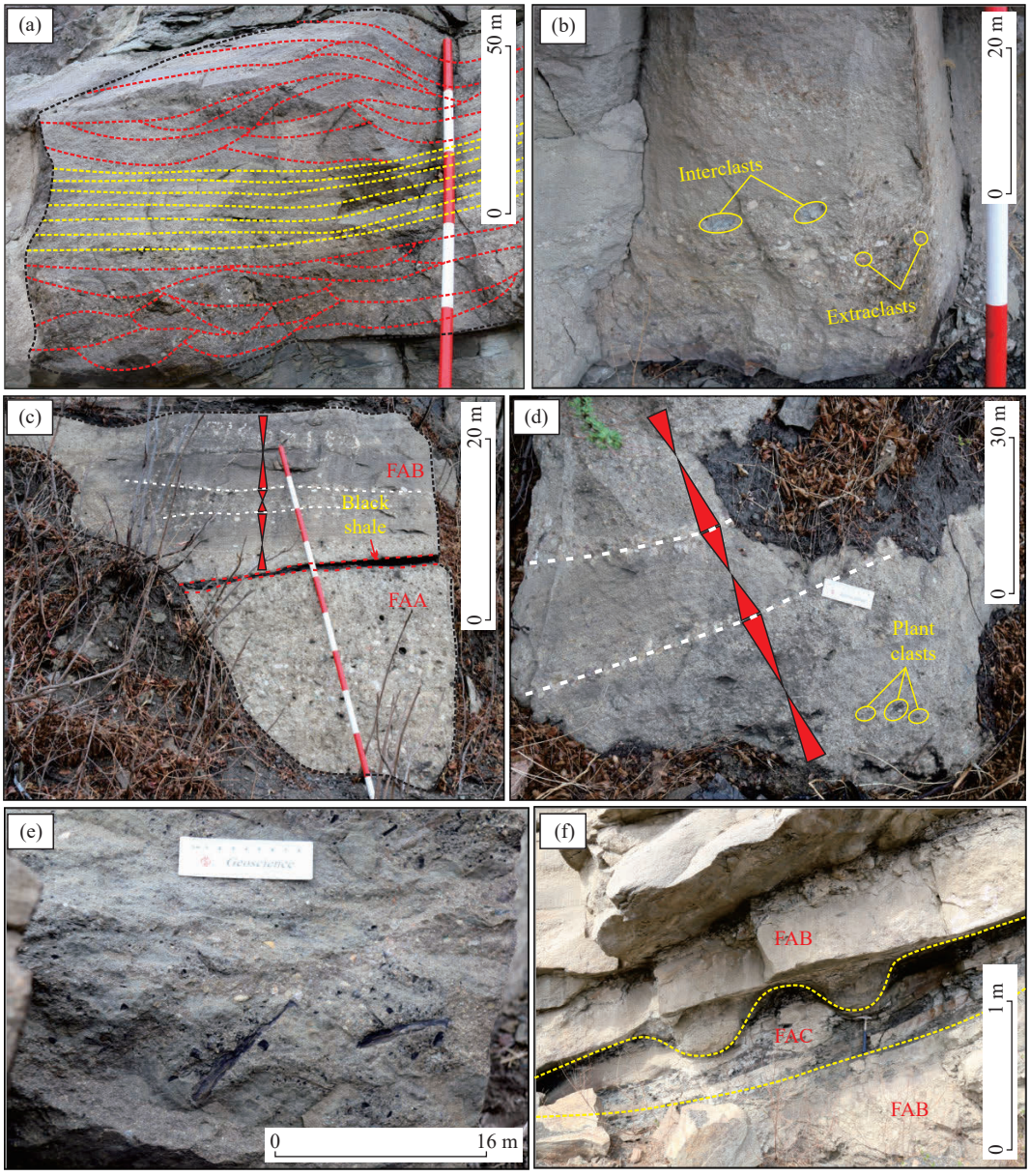

Fig. 3. FAB outcrop of middle branch channel deposits (modified from Yan DZ et al., 2020). a–sandstone with parallel bedding (F5), trough cross-bedding (F4) and cross-bedding (F4); b–red conglomerates are mixed with greyish-green mud pebbles; c–black shale serves as the boundary between FAA and FAB; d–complete vertical section of a single hyperpycnal flow deposition, with normal graded bedding, erosion surface, and reverse graded bedding; plant fragments and gravels in directional arrangement; e–a large amount of fragments; f–flute clasts at the bottom of FAB.

reflect the waxing-to-waning energy of flood hydrograph (Mulder T et al., 2001). Likewise, the alternative occurrences of cross bedding and parallel bedding reflect the hydrodynamics of an ordinary hyperpycnal flow. As the gravels are near the erosional surface, it is concluded that the hydrodynamics of the hyperpycnal flow was strong and then weak (Zavala C et al., 2006). In addition, according to the direction of the long axis of the gravels, it is inferred that the hyperpycnal flow was approximately SW-NE. A large number of plant fragments are found in FAB, representing that a large number of extrabasinal terrigenous clastics were deposited in the hyperpycnal flow deposits, which were transported from land by flood (Yang RC et al., 2015; Sun FN et al., 2016). In addition, there are many intraclasts, such as greyish-green mud pebbles. Flute casts observed at the bottom of FAB are another sign of hyperpycnal flow deposits, as Sun FN et al. (2016) considers them a good evidence of hyperpycnal flow.

4.3. Facies association C

Facies association C (FAC) is fine to silty sandstone and mudstone with thin horizontal bedding, and locally interbedded with deformed and layered sandstone (F7 to F8 in Table 1; Fig. 4). It should be noted that superimposition of normal graded bedding and reverse graded bedding are not observed in FAC. Also, sediments in FAC contain a large amount of terrestrial organic matter (Sun FN et al., 2016). The thickness of the thin sandstone and mudstone is around 0.2 m

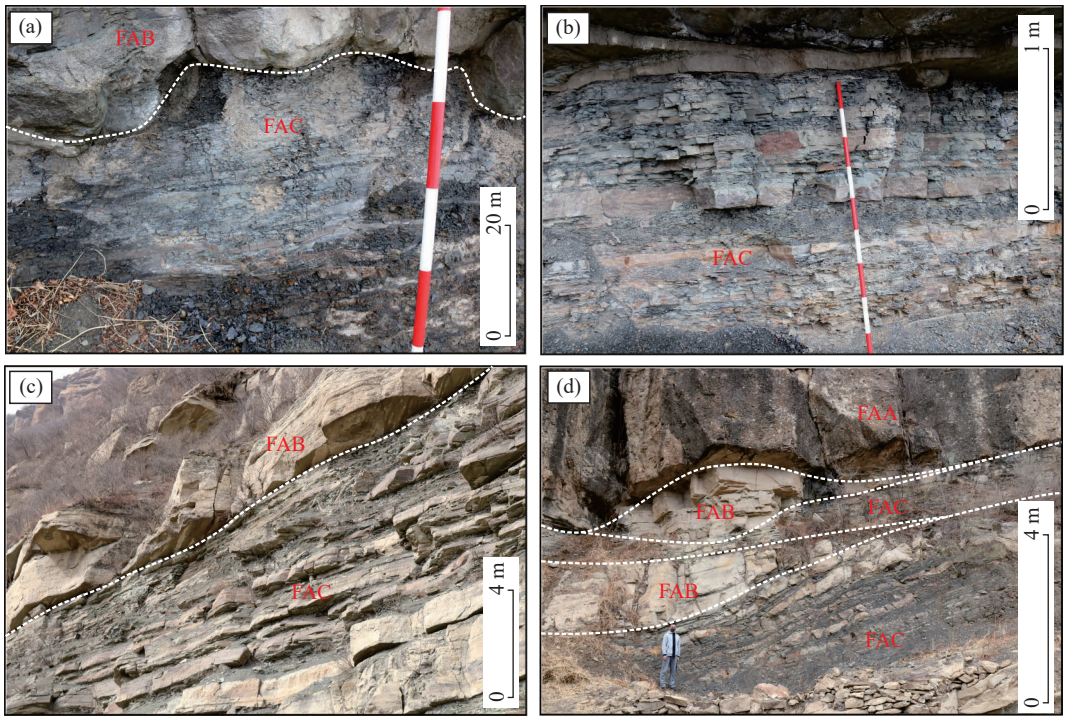

Fig. 4. Distal lobe deposits (FAC) (modified from Yan DZ et al., 2020). a–FAC eroded by overlying FAB; b–thin sandstone and mudstone; c–deformed structure; d– FAC contacts FAA and FAB, and eroded by overlying FAA and FAB.

to 0.5 m and 0.2 m to 1 m, respectively (Fig. 4b). The maximum thickness of FAC is up to 20 m in the Shangyuan outcrop. The sediments in FAC are smaller than FAA and FAB, observed in field. Deformed structures are locally observed in FAC (Fig. 4c). The sandstone layers in FAC are thinner than those in FAA and FAB, but the mudstone layers are thicker. The mudstone in FAC is generally dark grey and black, darker than those in FAA and FAB. On the vertical profile, FAC is always in contact with FAA and FAB, because of the erosion of FAA and FAB (Figs. 4a, d).

In comparison with FAA and FAB, the sediments in FAC are smaller, and have horizontal bedding, but no superimposition of normal bedding and reverse bedding. The depositional environment of FAC may be flat, located far from the source. As reported, the hyperpycnal flow should have been very slow when it reached the area where FAC was deposited (Zavala C et al., 2006; Sun FN et al., 2016). On the contrary, coarse sediments were deposited into FAA and FAB. Likewise, the horizontal bedding in FAC is the result from fine suspending sediments in the hyperpycnal flow. It can be concluded that FAC sediments are less cemented than FAA and FAB, since the sandstone-to-mudstone ratio is lower in FAC. Therefore, FAC sediments were easily eroded when overlying FAA and FAB were deposited, resulting in flute casts.

5. Depositional process of hyperpycnal flow deposits

When flooding, the density of the water rises substantially so that it may largely exceed the density of the original water (Mulder T et al. 2003). With flood into river, a hyperpycnal flow forms (Bates CC, 1953) (Fig. 5). The depositional process of hyperpycnal flow deposits is controlled by flood whose flowing rate increases first and then decreases (Woltemade CJ, 1994), so it can be divided into three phases: Acceleration, erosion and deceleration (Fig. 6).

In the acceleration phase, the hyperpycnal flow initially enters the basin nearby and then its rate gradually increases. Terrigenous debris originally carried by flood mixes with underwater debris, which indicates the original sediments in the basin become unstable and may be taken away by the hyperpycnal flow under its erosion power. Therefore, there are a lot of mixed deposits of red mud pebbles with gray mud pebbles (Fig. 2d). As the velocity of the hyperpycnal flow increases, a reverse grading bottom unit begins to accumulate (Fig. 6), resulting in the sedimentary structures caused by traction flow, such as cross, climbing and parallel beddings (Fig. 3a).

As the velocity of the hyperpycnal flow continues to increase, erosion starts, and the velocity of the hyperpycnal flow reaches its maximum, namely the flood peak. The eroding capacity of the hyperpycnal flow reaches the strongest, and the reverse grading basal unit deposited early is eroded, leaving eroded surfaces and waterways (Fig. 6). In addition, it's believed that during the acceleration phase, the hyperpycnal flow carries the sediments relatively coarse. Then in the deceleration phase, the coarser sediments deposit, making flowing velocity in the erosion stage inconsistent (Fig. 6). In the main channel deposits, only eroded surfaces and a normal grading top unit are observed, but no reverse grading unit (Fig. 2a). However, in the middle branch channel deposits, reverse grading is obvious (Figs. 3c, d). This sedimentary characteristic indicates that the deposits left in the acceleration stage suffered strong erosion in the main

Table 1. Description and interpretation of lithofacies (modified from Yan DZ et al., 2020).

Lithofacies	Picture	Textures	Structures	Bed thickness	Environments and processes
F1: Massive bedding conglomerate		Conglomerates (mixed colors, sub-round to angular, poorly sortable and round) in sandy matrix.	Massive bedding, imbricated structures, scours and fillings	20 cm to 40 cm each bed, 2 cm to 15 m in total	Main channels; near sources; coarse sediments (bedload), and fine sediments (free material). Flood enters the lake, and erodes main channels
F2: Massive bedding sandstone with gravels		Medium to coarse sandstone with gravels (sortable and round).	Massive bedding, charcoal	2 m to 8 m high bed sets, 15 cm to 32 cm each, and up to 1 m in total	Branch channels; coarse sediments (bedload), and fine sediments (free material). As the hyperpycnal energy wanes, and the slope becomes gentle, branch channels are created
F3: Graded bedding sandstone with gravels		Medium-coarse sandstone with several gravel (sortable and round) beds	Normal graded bedding and reverse graded bedding are superimposed, erosion surface, imbricated structures	20 cm to 80 cm each, amalgamated	Branch channels; coarse sediments (bedload), and fine sediments (free material). A single hyperpycnites has three depositional phases: acceleration, erosion-plus-bypass, and deceleration, which record the complete evolution of a sustainable hyperpycnal flow
F4: Trough cross-bedding sandstone		Medium-coarse sandstone with several gravel (directional, sortable and round) beds	Asymmetrical cross-bedding	15 cm to 100 cm each, 2 m to 6 m in total	Branch channels; coarse sediments (bedload), and fine sediments (free material); near sources and axial zones. Trough cross-bedding is more likely to form near the source and in the axial zone, because the flow velocity reaches its maximum at these zones
F5: Parallel bedding sandstone		Medium-coarse sandstone	Planar laminations with distinct lamina boundaries, water-escaping structure	20 cm to 40 cm each, 2 m to 6 m in total	Branch channels; far from sources and axial zones. Parallel bedding is more likely to form at the zone far away from the source and at the axial zone, because the flow velocity slows down
F6: Climbing bedding sandstone		Medium-coarse sandstone	Asymmetrical cross lamination with climbing set boundaries	1 m to 2 m high bed sets, composed of 10 cm to 20 cm thick beds	Branch channels; at the edge of the channel. Climb bedding is more likely to form at the zone far away from the source and at the edge of the channel, because the flow velocity is very slow there
F7: Horizontal bedding sandstone	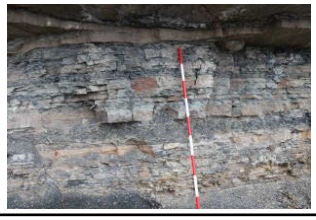	Fine to silty sandstone	Horizontal bedding	10 cm to 20 cm and interbedded with horizontal mudstone, 1 m to more than 20 m in succession	Lobe deposition; suspended sediments from dilute turbidity currents

Table 1. (*Continued*)

Lithofacies	Picture	Textures	Structures	Bed thickness	Environments and processes
F8: Horizontal bedding mudstone		Clay to silt	Horizontal bedding, blocky greenish grey to black	15 cm to 30 cm and interbedded with horizontal sandstone, 1 m to more than 20 m in succession	Lobe deposition; suspended sediment from dilute turbidity currents

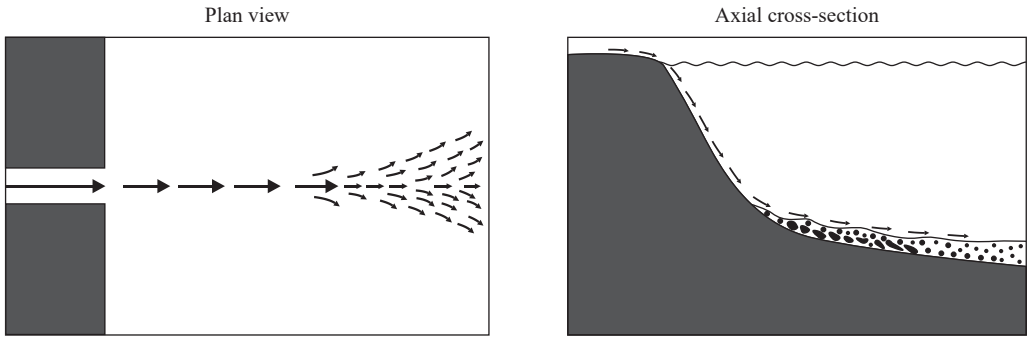

Fig. 5. Schematic diagram of the hyperpycnal flow into basin (after Bates CC, 1953).

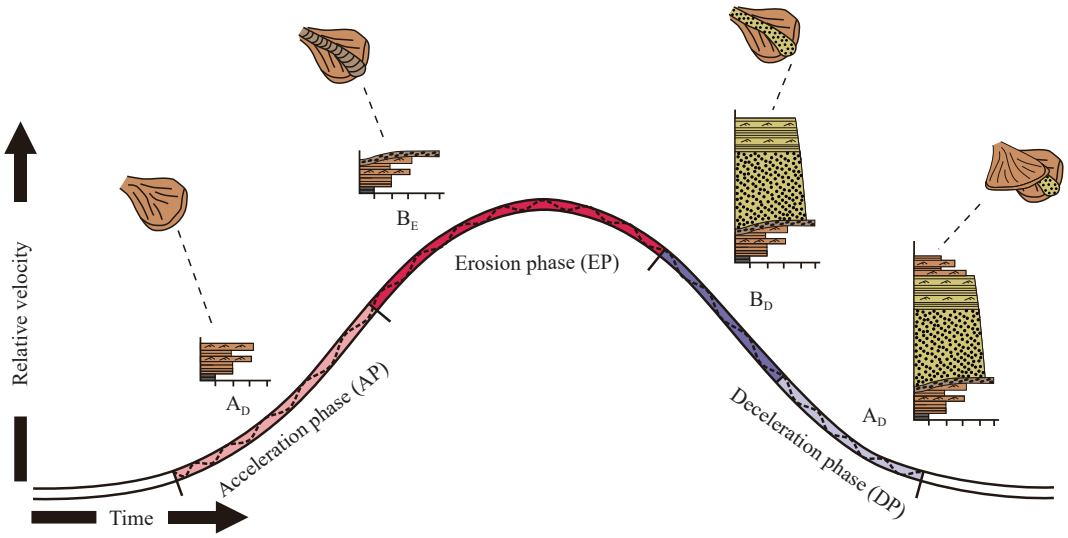

Fig. 6. Flood hydrograph and associated sequence of hyperpycnal flow. "A" means deposit from low-velocity flood (low-density hyperpycnal flow). "B" means deposits from high-velocity flood (high-density hyperpycnal flow). The subscripts D and E refer to depositional and erosional flows respectively. The black dashed line shows the fluctuation of flood flow velocity.

channel. As the distance from the source increases, the velocity and concentration of the hyperpycnal flow decreases, so its erosion ability is gradually weakened. As a result, the reverse-grading deposits are preserved in the middle branch channel, but eroded in the proximal channel.

As the velocity of the hyperpycnal flow decreases, the deposits carried by it fill in the waterways, leaving waterway deposits (Fig. 6). In the middle branch channel, the authors found a special sedimentary structure. It is the alternating occurrences of cross bedding and parallel bedding (Fig. 7). This phenomenon shows that, although hyperpycnal flow has a general tendency to increase first and then decrease, the flowing velocity is also in a state of continuous fluctuation (Fig. 6). As the distance from the deposit source increases, the deposits gradually become finer. The deposits in the proximal main channel are coarse, poorly sortable and round. In comparison, those in the middle branch channel and the distal lobe are fine, and well sortable and round. In addition, since the velocity of the fluid front is slow, the deposits in the distal lobe are not obviously normal or reverse grading. Judging from the directional gravels preserved near the erosion surface, it's believed that the direction of the hyperpycnal flow was SW-NE. After the erosion stage, it's the deceleration stage, during which the velocity of the hyperpycnal flow started to decrease, until it was completely deactivated. The normal grading top unit, which covers the previous deposits,

is another evidence of the slowing down hyperpycnal flow. The thick mudstone layer covering the sand body indicates the end of the depositional process of the hyperpycnal flow. The presence of thin sand and mud interbeds also indicates that flocculating occurred during the deposition of the distal lobe (Fig. 4d). At the same time, the authors discovered a special depositional phenomenon. There isn't plant debris in the proximal main channel, but a lot in the middle branch channel and the distal lobe (Fig. 3e). Based on this sedimentary feature, it's inferred that after entering the lake basin, the hyperpycnal flow was supported by the lake water to produce lofting plumes (Fig. 8). When the hyperpycnal flow initially entered the basin, its velocity was fast, so that it's difficult for plant debris to deposit and be preserved. As moving farther, the hyperpycnal flow gradually slowed down. At the same time, under the jacking effect of the lake or sea water, plumes were produced in the front of the hyperpycnal flow, so that a large amount of plant debris were preserved in the distal lobe and the middle branch channel (Fig. 8).

Based on the depositional process, the authors established a depositional process model (Fig. 9). According to this model, the authors demonstrated that the depositional process can be divided into three stages, namely acceleration, erosion and deceleration. During the acceleration stage, reverse grading deposits appeared. However, in the erosion stage, they were eroded by the hyperpycnal flow and became thinner or even disappeared. Finally, in the deceleration stage, normal grading deposits covered early deposits, resulting in the special sedimentary characteristics shown by superimposition of reverse and normal grading deposits.

By comparing with previous research results, the authors found that marine hyperpycnites have obvious bedding variation rules. For example, according to Zavala's study in 2006, the sediments left by the hyperpycnal flow in the acceleration stage mainly developed climbing bedding and parallel bedding, the sediments formed in the erosion stage were denudated into surfaces, and the sediments formed in the deceleration stage mainly developed through cross-bedding and parallel bedding and climbing bedding (Zavala C et al., 2006; Fig. 10). The variation of bedding types reflects the variation law of the hydrodynamic force first increasing and then decreasing. However, there is no obvious change of bedding types in lacustrine hyperpycnites, which is mainly manifested by the change of grain size (Fig. 9). The authors believe that the difference in characteristics of marine and lacustrine hyperpycnites is mainly due to the long duration of flood controlling the formation of marine hyperpycnites, large basin capacity, and obvious sediment differentiation. Therefore, marine hyperpycnites have sufficient time and space to develop obvious bedding, and the rule of obvious bedding is observable. The flood duration controlling the formation of lacustrine hyperpycnites is short, the capacity of the lake basin is relatively small, and the sediment differentiation is not obvious, so the variation characteristics of lacustrine hyperpycnites are mainly reflected by grain size, but the bedding variation is not obvious.

6. Conclusions

The outcrop of hyperpycnal flow deposits caused by flood implies that the internal architecture of hyperpycnites is produced in a complete cycle of hyperpycnal flow. During the waxing stage, reverse grading deposits appear, but they are locally or completely reworked during the erosion stage. Subsequently, during the waning stage, normal grading deposits cover early deposits, resulting in the special sedimentary characteristics shown by superimposed reverse and normal grading. With successive hyperpycnal events, the

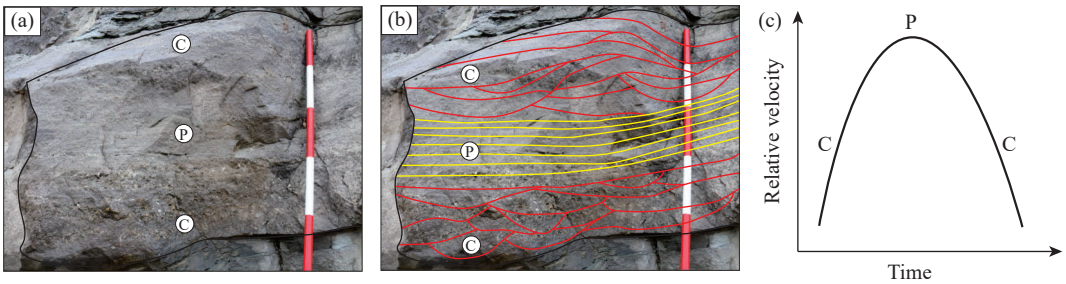

Fig. 7. a–Photograph of an event bed of FAB on Sangyuan section; b–schematic drawing of an event bed, interpreted from one fluctuation of hyperpycnal flow, showing initial deposition of trough cross-bedding (C) in sandstone, then higher-energy bed (P) in sandstone, and finally trough cross-bedding (C) in sandstone; c–hypothetical flood hydrograph that generates a hyperpycnal flow.

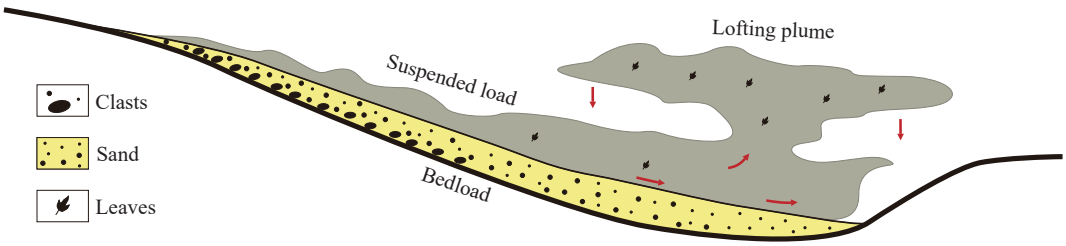

Fig. 8. Hyperpycnal flow with extrabasinal-derived bedload common in proximal zones characterized by high shear forces and in distal zones characterized by lofting plume.

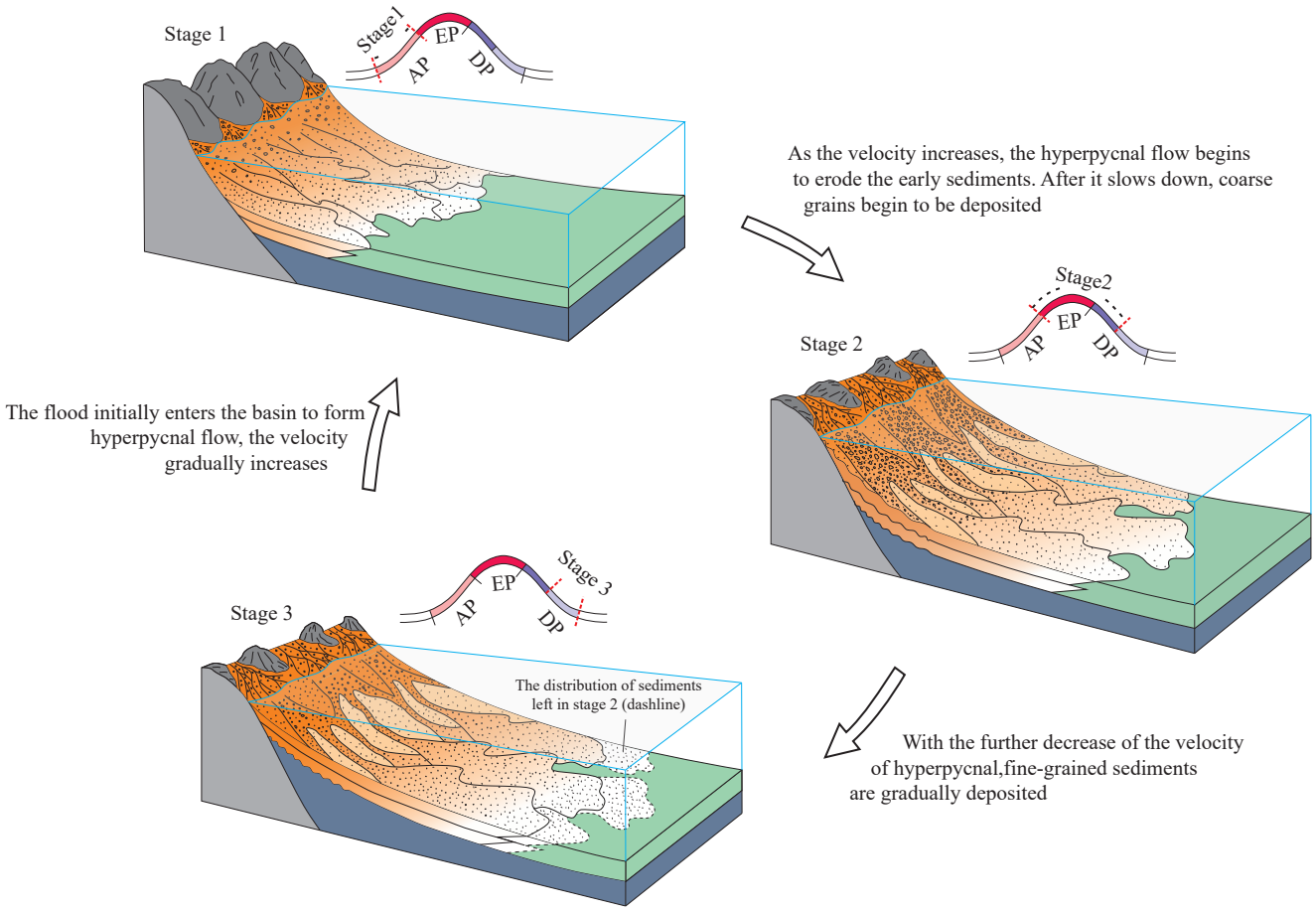

Fig. 9. Conceptual model explaining the depositional process of hyperpycnal flow. In Stage 1, when flood initially enters the lake basin, it becomes a hyperpycnal flow at a slow and then gradually increasing velocity, resulting in reverse grading sediments (Fig. 6). In Stage 2, with the increase of the velocity of the hyperpycnal flow, it begins to erode early sediments and creates channels. As the velocity decreases, coarse sediments are deposited and fill in the channels in a normal grading manner. Stage 2 covers erosion and early deceleration (Fig. 6). After entering Stage 3, the hyperpycnal velocity further decreases, and fine sediments are gradually deposited in distal lobes (Fig. 6).

strong scouring effect of the hyperpycnal flow makes the hyperpycnites have the sedimentary characteristics of terrestrial debris mixing with underwater debris. And under the jacking effect of the lake water, plumes are produced in the front of the hyperpycnal flow, so that a large amount of plant debris is preserved in the distal lobe and the middle branch channel, but no plant debris in the proximal main channel.

CRediT authorship contribution statement

De-zhi Yan: Methodology, investigation, validation, writing – original draft, visualization. Ru-kai Zhu: Resources, data curation, supervision, project administration. Hao Shou: Resources, data curation, supervision, project administration. All authors discussed the results and contributed to the final manuscript.

Declaration of competing interest

The authors declare no conflicts of interest.

Acknowledgment

The authors are grateful to the editor and anonymous reviewers for very constructive and useful comments. The authors are also thankful for permission to publish this paper from the Scientific research and technology development project of PetroChina (2021DJ5303).

References

Bates CC. 1953. Rational theory of delta formation. AAPG Bulletin, 37, 2119–2162.

Cao YC, Wang SJ, Wang YZ, Li WQ, 2017. Sedimentary characteristics and depositional model of slumping deep-water gravity flow deposits: A case study from the middle Member 3 of Paleogene Shahejie Formation in Linnan subsag, Bohai Bay Basin. Journal of Palaeogeography, 19, 419–432. doi: 10.7623/syxb201706001.

Cope T. 2003. Sedimentary Evolution of the Yanshan Fold-Thrust Belt, Northeast China. Stanford University, 123–144.

Cope T, Luo P, Zhang XY, Zhang XJ, Song JM, Zhou G, Shultz RM. 2010. Structural controls on facies distribution in a small half-graben basin: Luanping basin, northeast China. Basin Research. 22, 33–44. doi: 10.1111/j.1365-2117.2009.00417.x.

Dadson S, Hovius N, Pegg S, Dade WB, Horng MJ, Chen H. 2005. Hyperpycnal river flows from an active mountain belt. Journal of Geophysical Research: Earth Surface, 110 (F4).

Er C, Gu JY, Niu JY, Cheng N, Han SF. 2010. Gravity-Driven Processes: A more important transport mechanism of deposits in Xiguayuan Formation of Lower Cretaceous in Luanping Basin,

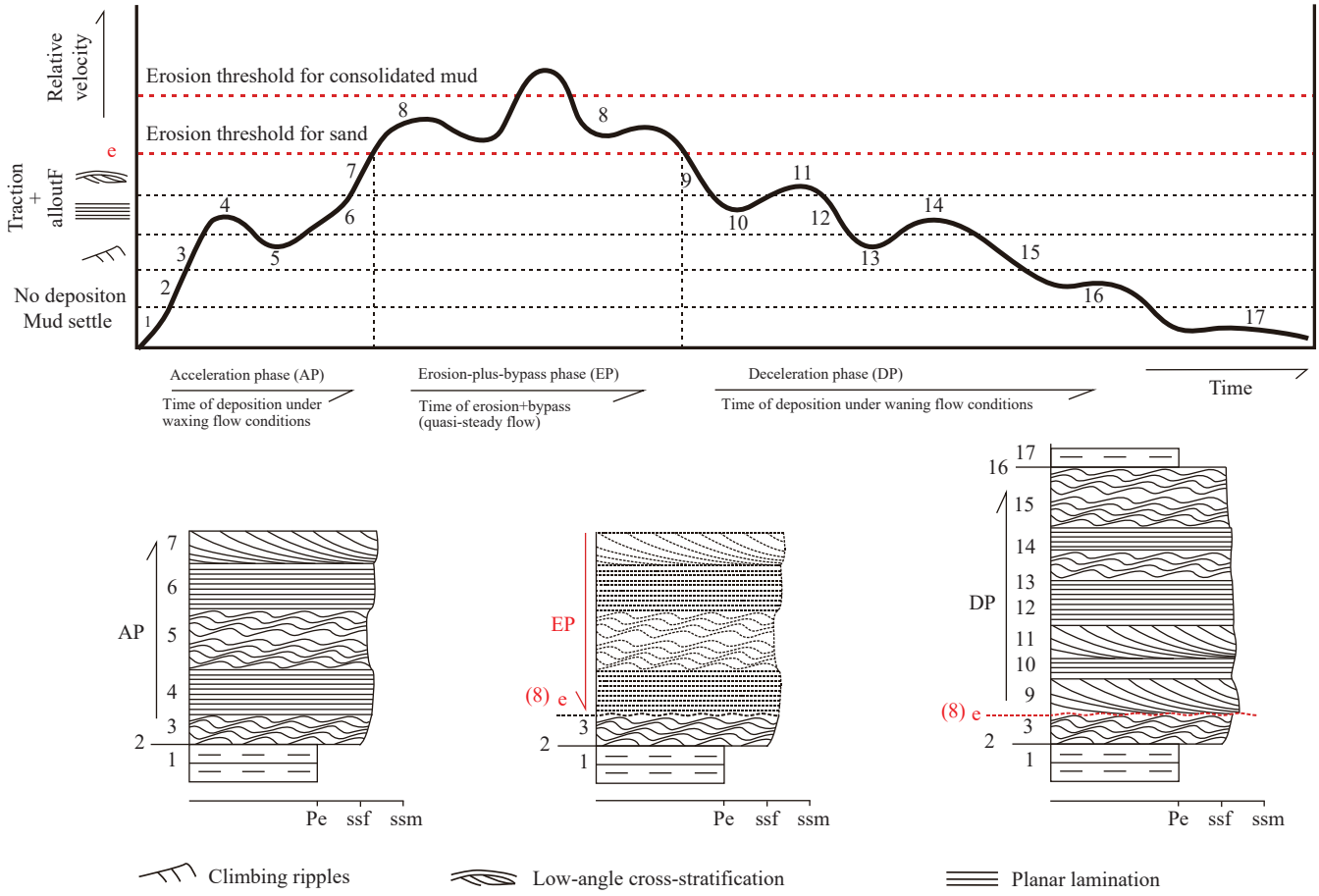

Fig. 10. Hypothetical diagram showing a curve of fluctuating velocity of a quasi-steady underflow and its consequences for sedimentation at a fixed point in a basin (modified from Zavala C, 2006). Three main phases are recognized. Acceleration phase (AP): Accumulation of intervals 1 to 7 by an accelerating and fluctuating flow. Erosion-plus-bypass phase (EP): Erosion of some of the preceding deposits. Deceleration phase (DP): Accumulation of intervals 9 to 15 from a decelerating and fluctuating flow.

Northern Hebei. Geological Review, 56(3), 312–320.

Henstra GA, Grundvåg SA, Johannessen EP, Kristensen TB, Midtkandal I, Nystuen JP, Rotevatn A, Surlyk F, Sæther T, Windelstad J. 2016. Depositional processes and stratigraphic architecture within a coarse-grained rift-margin turbidite system: The Wollaston Forland Group, east Greenland. Marine and Petroleum Geology, 76, 187–209. doi: 10.1016/j.marpetgeo.2016.05.018.

Khan SM, Imran J, Bradford S, Syvitski J. 2005. Numerical modeling of hyperpycnal plume. Marine Geology, 222, 193–211.

Lamb MP, Mohrig D. 2009. Do hyperpycnal-flow deposits record river-flood dynamics? Geology, 37(12), 1067–1070. doi: 10.1130/G30286A.1.

Li Y. 2003. Fan- delta depositional systems of Xiguayuan Formation in Luanping Basin. Acta Geoscientia. Sinica, 24, 353–356.

Lowe DR. 1982. Sediment gravity flows: II. Depositional models with special reference to the deposits of high-density turbidity currents. Journal of Sedimentary Petrology, 52, 279–297.

Middleton GV, Hampton MA. 1973. Sediment gravity flows: Mechanics of flow and deposition. In: Middleton GV, Bouma AH (Eds.), Turbidites and Deep-Water Sedimentation. Society of Economic Paleontologists and Mineralogists Special Publication, 1–38.

Middleton GV. 1976. Hydraulic interpretation of sand size distributions. The Journal of Geology, 84, 405–426. doi: 10.1086/628208.

Mulder T, Migeon S. 2001. Twentieth century floods recorded in the deep Mediterranean sediments. Geology, 29, 1011–1014. doi: 10.1130/0091-7613(2001)029<1011:TCFRIT>2.0.CO.

Mulder T, Syvitski JPM, Migeon S, Faugeres JC, Savoye B. 2003. Marine hyperpycnal flows: Initiation, behavior and related deposits: A review. Marine and Petroleum Geology, 20, 861–882. doi: 10.1016/j.marpetgeo.2003.01.003.

Parsons JD, Bush JWM, Syvitski JPM. 2001. Hyperpycnal plume formation from riverine outflows with small sediment concentrations. Sedimentology, 48, 465–478. doi: 10.1046/j.1365-3091.2001.00384.x.

Peter AL, Steel RJ. 2006. Hyperpycnal flow variability and slope organization on an Eocene shelf margin, Central Basin, Spitsbergen. AAPG bulletin, 90(10), 1451–1472. doi: 10.1306/04240605144.

Pierdomenico M, Casalbore D, Chiocci FL. 2019. Massive benthic litter funnelled to deep sea by flash-flood generated hyperpycnal flows. Scientific Reports, 9(1), 1–10. doi: 10.1038/s41598-019-41816-8.

Shanmugam G. 2019. Slides, slumps, debris flows, turbidity currents, hyperpycnal flows, and bottom currents. In: Cochran JK, Bokuniewicz HJ, Yager PL (Eds). Encyclopedia of ocean sciences, 3rd edn. San Diego, Academic Press, 228–257. doi: 10.1016/B978-0-12-409548-9.10884-X.

Shanmugam G. 2000. Deep-water processes and facies model: A critical perspective. Marine and Petroleum Geology, 17(2), 285–342. doi: 10.1016/S0264-8172(99)00011-2,.

Soyinka OA, Slatt RM. 2008. Identification and micro-stratigraphy of hyperpycnites and turbidites in cretaceous lewis shale, Wyoming. Sedimentology, 55, 1117–1133. doi: 10.1111/j.1365-3091.2007.00938.x.

Sun FN, Yang RC, Li DY. 2016. Research progresses on hyperpycnal flow deposits. Acta Sedimentologica Sinica, 3, 452–462.

Walker RG. 1978. Deep-water sandstone facies and ancient submarine fans-models for exploration for stratigraphic traps. The American

Association of Petroleum Geologists, 62, 932–966. doi: 10.1306/C1EA4F77-16C9-11D7-8645000102C1865D.

Warrick JA, Milliman JD. 2003. Hyperpycnal sediment discharge from semiarid southern California rivers: Implications for coastal sediment budgets. Geology, 31(9), 781–84. doi: 10.1130/G19671.1.

Woltemade CJ. 1994. Form and process: Fluvial geomorphology and flood-flow interaction, Grant River, Wisconsin. Annals of the Association of American Geographers, 84(3), 462–479. doi: 10.1111/j.1467-8306.1994.tb01870.x.

Wu FD, Chen YJ, Hou YA, Zhang F, Li Y. 2004. Characteristics of sedimentary tectonic evolution and high-resolution sequence stratigraphy in Luanping Basin. JournaI of China University of Geosciences. 29, 625–630.

Xian BZ, Wang JH, Gong CL, Yin Y, Chao CZ, Liu JP, Zhang GD, Yan Q. 2018. Classification and sedimentary characteristics of lacustrine hyperpycnal channels: Triassic outcrops in the south Ordos Basin, central China. Sedimentary Geology, 368, 68–82. doi: 10.1016/j.sedgeo.2018.03.006.

Yan DZ, Xu HM, Xu ZH, Lei ZC, Tian M, Cheng L, Ma YH, Wang ZL, Ostadhassan M. 2020. Sedimentary architecture of hyperpycnal flow deposits: Cretaceous Sangyuan outcrop, from the Luanping Basin, North East China. Marine and Petroleum Geology, 121, 104593. doi: 10.1016/j.marpetgeo.2020.104593.

Yang RC, Jin ZJ, Sun DS, Fan AP. 2015. Discovery of hyperpycnal flow deposits in the Late Triassic Lacustrine Ordos Basin. Acta Sedimentologica Sinica, 33(1), 10–20. doi: 10.14027/j.cnki.Cjxb.2015.01.002.

Zavala C, Ponce JJ, Arcuri M, Drittanti D, Freije H, Asensio M. 2006. Ancient lacustrine hyperpycnites: A depositional model from a case study in the Rayoso Formation (Cretaceous) of West-Central Argentina. Journal of Sedimentary Research, 76, 41–59. doi: 10.2110/jsr.2006.12.

Zavala C, Arcuri M. 2016. Intrabasinal and extrabasinal turbidites: Origin and distinctive characteristics. Sedimentary Geology, 337, 36–54. doi: 10.1016/j.sedgeo.2016.03.008.

Zavala C, Pan SX. 2018. Hyperpycnal flows and hyperpycnites: Origin and distinctive characteristics. Lithologic Reservoirs, 30(1), 1–18. doi: 10.3969/j.issn.1673-8926.2018.01.001.

Zavala C. 2020. Hyperpycnal (over density) flows and deposits. Journal of Palaeogeography, 9, 1–21. doi: 10.1186/s42501-020-00065-x.

Zhang YL, Qu HJ, Meng QR. 2007. Depositional process and evolution of Luanping Early Cretaceous basin in the Yanshan structural belt. Acta Petrologica Sinica, 23, 667–678.

Zou CN, Wang L, Li Y, Tao SZ, Hou LH. 2012. Deep-lacustrine transformation of sandy debrites into turbidites, Upper Triassic, Central China. Sedimentary Geology, 265/266, 143–155. doi: 10.1016/j.sedgeo.2012.04.004.